Applied Chemical Engineering (2026) Volume 9 Issue 2 ISSN: 2578-2010 (O)
doi: 10.59429/ace.v9i2.5932

RESEARCH ARTICLE

Comparative Cloud Point Extraction of Gold Using Novel Benzimidazole vs. Benzothiazole Azo-Ligands: Analytical Performance and Antibacterial Activity

Dalal Abbas Ali*, Ibtehaj Raheem Ali

Department of Chemistry, College of Education for Women, University of Kufa, Iraq

***Corresponding author:** Dalal Abbas Ali; dalala.alyousefi@student.uokufa.edu.iq

ABSTRACT

Herein, two new azo reagents, 2-[(1-banzimidazol)azo]-2-hydroxy-5-banzal (BIApB) and 6-[(1-banzethiazol) azo thymol] (BTAT), were synthesized and identified using FTIR, UV-Vis, mass spectrometry, and ^{1}H-NMR. Also, this research presents a comparative analysis of novel azo-chelating reagents for the cloud point extraction (CPE) of gold complexes. The study evaluates how the structural differences between the benzimidazole and benzothiazole moieties influence both extraction efficiency (E%) and the biological potency of the resulting complexes. The optimal conditions for both reagents (BIApB and BTAT) were determined. These included pH, TritonX-100 concentration, temperature, and heating time. The thermodynamic characteristics of the CPE were calculated for both chelators with gold. The CPL layer easily removed by syringe.

This approach indicates an endothermic reaction. The analytical figures for BIApB and BTAT, respectively, were good, with limits of detection (LOD) of 0.30 and 0.35 µg L^{-1}, limits of quantities (LOQ) of 1.0 and 1.16 µg L^{-1}, pre-concentration factors (PF) of 200 and 125, enrichment factors (EF) of 125 and 147.4, and RSD% values of 8.7% and 1.1%. The calibration curves for two complexes were linear from 1.0 to 7.0 µg L^{-1}.

Additionally, analytical results confirm effective gold recovery with both reagents; however, antibacterial screening against E. coli and S. aureus revealed that the BTAT-Au(III) complex possesses significantly higher bioactivity, with inhibition zones reaching 28 mm. This is attributed to the increased lipophilicity provided by the sulphur-containing benzothiazole ring, which facilitates membrane penetration. Statistical t-tests ($p < 0.05$) confirmed that the antibacterial effects are dose-dependent, establishing BTAT as a high-performance, multifunctional reagent for both trace metal analysis and antimicrobial applications.

Keywords: gold, benzothiazole, benzimidazole, azo-ligands, antibacterial activity, cloud point extraction, Surfactant-based extraction.

ARTICLE INFO

Received: 9 March 2026
Accepted: 13 May 2026
Available online: 18 June 2026

1. Introduction

One of the best elements in the world, gold has nearly always improved industry fields. As a result, gold now has a significant role in modern industrial and medicinal traditions [1,2]. Additionally, its products are essential to many scientific and technological domains, such as the petrochemical, dental care, cosmetic, jewellery, nuclear power, and computer industries [3]. Additionally, studies suggest that gold may have anti-aging properties. Gold is an environmentally safe metallic substance with numerous uses; thus, determining its trace level in genuine samples using a rapid, precise, simple, sensitive, and repeatable procedure is important [4-6]. Several direct methodologies were used to determine gold in actual specimens. Most of these detectors were Inductively Coupled Plasma Mass (ICP-MS) or Atomic

Emission (ICP-AES) spectrometers [7-9]. The Ultraviolet-Visible Spectrophotometer (UV-Vis) [10] and Neutron Activation Analysis (NAA) [11].

In the past few years, Cloud Point Extraction (CPE) approaches were introduced to address the previous limitations. These methods used surfactants (micelles) as extractants [12-15]. CPE is a well-established green method that uses the fogging behavior of non-ionic surfactants at high temperatures to efficiently separate and preconcentrate trace metal ions. CPE reduces the usage of harmful organic solvents while providing important benefits over traditional extraction systems, such as speed, selectivity, and high enhancement ability[16,17]. Based on the CPE mechanism, the surfactant amounts must exceed their critical micelle concentrations (CMC). They were required increasing the temperature above the critical temperature (CT) [18]. This elevated temperature induces the creation of a cloud point layer (CPL), which is the result of dehydration due to the micelles' polar surface. The CPL can be distinguished by its reduced volume as compared to an aqueous phase in which the analytes of interest are already preconcentrated. The three simple processes are phase separation, cloud formation, and analyte solubilization [19-22]. These steps are crucial for applying CPE techniques to separate or preconcentrate the analytes. The partition of analyte between the CPL and the water-rich layer starts above the CT. Also, the CPL serves as the organic layer connected to the solvent extraction. Micelles' separation in water was affected by both internal energy and entropy. Furthermore, the inter-micellar interaction potential influences phase separation at lower critical solution temperatures. The interaction potential is repulsive at low temperatures and has a deleterious effect at high temperatures [23,24].

The present study introduces two synthesis ligands, (BIApB, and BTAT), were designed and identified to cause clouding in Triton X-100 systems at specific temperatures. This technique was effectively used to determine gold as an ion-pair-associated complex, with chelators ensuring efficient metal transfer to the organic layer. This study shows that BIApB and BTAT are capable of extraction of Au (III) in conjunction with well-known ligands, providing a straightforward, effective, and green technique for their preconcentration and characterization. The optimal parameters for CPE were established. Beyond extraction performance, the study evaluated the biological activity of the complexes against *Escherichia coli* and *Staphylococcus aureus*. Results indicated that both reagents facilitated effective gold recovery. The BTAT-Au(III) complex demonstrated markedly superior antibacterial efficacy compared to the BIApB complex, which showed no activity against *E. coli*.

2. EXPERIMENTAL

Apparatus

Throughout this investigation, the absorption spectra of all reagents and complexes are scanned utilizing a Shimadzu double beam UV-Vis spectrophotometer model UV-1700 (Japan) with a 10-mm optical path cell, a spectral bandwidth of 1 nm (190 to 900 mm), and a wavelength of 190 – 1100 nm (±0.3 nm accuracy at the D2 peak of 656.1 nm, 486.0 nm, and ±0.1 repeatability). FTIR-8400S, Shimadzu (Japan Nuclear), CHN/O Analyzer, TRIUP International Corp-TRUV. The Nuclear Magnetic Resonance Spectrometer-HNMR (Bruker, 500 Hz Laboratory of Tehran University, Iran). The pH meter (Listed, Lab Equipment Co., E163694, CE, Germany). Thus, Electrical Balance Company Limited, Dool, CE, HR200, Japan, and Water Bath with Regulator (Hamburg 90), England, are used for heating.

Chemicals and reagents

All analytical reagents were bought from different vendors. All of the substances were used without prior purification. The standard, reagents, and samples are diluted with double-distilled water. The surfactant Triton X-100, chemical structure $C_8H_{17}C_6H_4(OC_2H_4)_n$ with n = (9-10), was obtained from Sigma (Sigma Ultra, >99.6%) and is used without extra purification. CDH (UK) supplied 99% NaOH, 37% HCl, and 99% $NaNO_2$. In a volumetric flask, dissolve 0.1 g of $NaAuCl_4.2H_2O$ (Merck, 99.97%) in 25 mL of water to obtain

an Au (III) standard solution (1 mg/mL). To prepare 1×10^{-2} M BIApB and BTAT solutions, dissolve 0.0266 g and 0.0310 g, respectively, in water and add 5.0 drops of Triton X-100.

Synthesis of 2-[(1-banzimidazol)azo]-2-hydroxy-5-banzal (BIApB) and Synthesis of 6-[(1-banzethiazol) azo thymol] (BTAT) reagents

To synthesize the novel ligands BIApB and BTAT, a similar diazotization and coupling procedure was employed [25,26]. The 0.02 mol of the starting amine (2.6632 g of 1H-benzo[d]imidazol-2-amine for BIApB and 3.0244 g of benzo[d]thiazol-2-amine for BTAT) was dissolved in an acidic aqueous solution. Then, every solution reacted with $NaNO_2$ at 0° C to form the diazonium salt. After 15 minutes, every solution was added slowly to an alkaline ethanol solution containing 0.02 mol of the coupling agent (2.4424 g of 4-hydroxybenzal for BIApB or 3.0044 g of thymol for BTAT), resulting in a brown precipitate. After 24 hours, the mixtures were diluted with chilled water, neutralized to pH 7 with HCl, filtered, washed, and purified via recrystallization from hot absolute ethanol and drying over $CaCl_2$. While both reagents are soluble in organic solvents like DMF, acetone, and ethanol but insoluble in water. These reagents were dissolved in water after adding 5.0 drops of Triton X-100. Also, they differ in their chemical properties: BIApB ($C_{14}H_{10}N_4O_2$, MW: 266.246 g mol^{-1}) has a melting point of 159 – 162 ° C, whereas BTAT ($C_{17}H_{17}SN_3O$, MW: 310.39 g mol^{-1}) melts at 218 – 221 ° C. The steps of these reactions were shown in **Figure 1 (A and B)**. These ligands were characterized by FTIR and UV-Vis. Also, the spectra of MS (S1, S2) and ^{1}HNMR (S3, S4) were shown in the supported file.

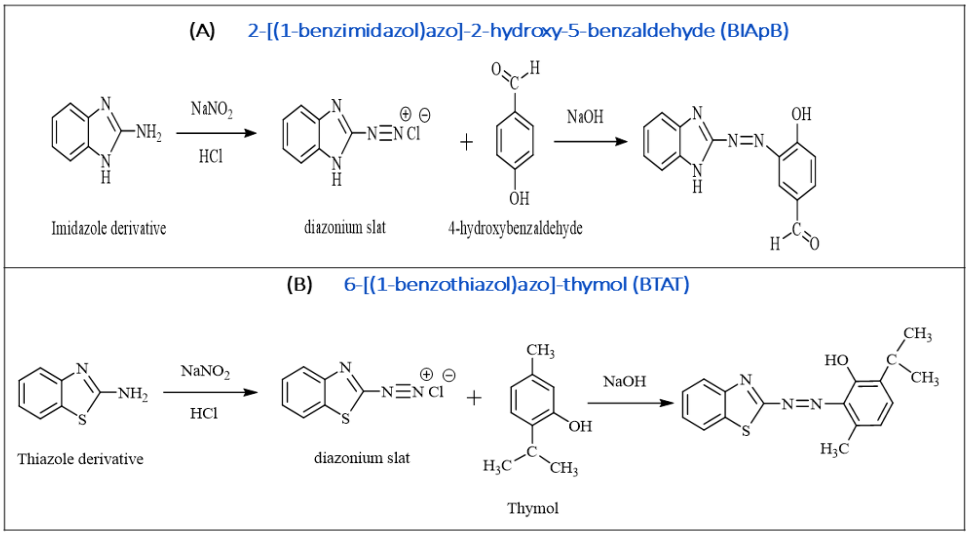

Figure 1. Schematic representation of the chemical synthesis routes for the novel azo ligands: (A) Synthesis of *2-[(1-banzimidazol)azo]-2-hydroxy-5-banzal (BIApB)* via diazotization of imidazole and coupling with 4-hydroxybenzal. (B) Synthesis of *6-[(1-banzethiazol) azo thymol] (BTAT)* via diazotization of benzothiazole and coupling with thymol.

2.1. The general CPE Procedure

To determine the Au (III) content in standard and sample solutions, 10 mL of the analyte (20 µg L^{-1}) of Au (III) was mixed with a 1×10^{-4} M concentration of either the BIApB or BTAT ligand. The solution acidity was strictly controlled to ensure optimal complexation, set at pH 10 for BIApB and pH 8 for BTAT. Following pH adjustment, Triton X-100 was added as the non-ionic surfactant, using 0.5 mL for the BIApB system and 0.8 mL for the BTAT system. The resulting mixture was placed in a thermostatic bath and heated at 80° C for 15 minutes to induce the cloud point. During this stage, the CPL containing the gold complex became highly viscous and separated from the bulk aqueous solution. CPL was completed by decanting the aqueous phase, notably achieving this result without the need for centrifugation or cooling. The CPL layer easily removed by syringe.

For the final analysis, the viscous CPL was dissolved in 5.0 mL of ethanol to reduce viscosity and facilitate measurement. The absorbance was measured using a 1 cm cell against a reagent blank prepared under optimal conditions without metal ions, with detection wavelengths set at λ_{max}= 584 nm for the Au-BIApB complex and λ_{max}= 526 nm for the Au-BTAT complex. Finally, the concentration of Au (III) in the aqueous phase was determined via flame atomic absorption spectroscopy (FAAS) using a standard calibration curve to calculate the distribution ratio (D).

2.2. Antibacterial Evaluation

The antibacterial effects of the produced azo derivatives BIApB, BTAT, and their complexes were determined using the diffusion technique with agar wells. Every sample of pathogenic bacteria isolates was made carefully by inoculating them into sterile Mueller-Hinton broth containers and incubating them for a day at 37° C. The liquid bacterial cultures were swab-inoculated on sterile Mueller-Hinton agar plates. Using a 6.0 mm sterile gel borer, holes were made into swab-inoculated dishes and labelled. The specimens were evaluated against two kinds of bacteria: Gram-positive Staphylococcus aureus MTCC-7443 and Gram-negative Escherichia coli MTCC-7410. These organisms, S. aureus and E. coli, were chosen as test organisms due to their ease of manipulation in the lab, unique biological traits, and extensive significance in people and animals. The amount of inoculum was reduced to 5×10^5 CFU/mL in a sterile saline solution. Samples of 10 µg/mL were dissolved in DMSO as a stock solution and loaded at different quantities ranging from 200 µg to 800 µg into various wells. DMSO (10%) served as a negative control. Furthermore, the results of the named azo derivatives were measured in terms of the zone of inhibition in millimeters [27,28].

3. RESULTS AND DISCUSSION

3.1. Spectral analysis

This study produced two dispersed azo dyes, termed BIApB and BTAT, using a simple diazo coupling technique at temperatures ranging from 0° C to 5° C. The produced azo compounds had yields ranging from 80% to 87%, showing a relatively good synthesis efficiency. Several spectroscopic approaches were used to validate the structural integrity of these azo compounds.

The FTIR spectrum of BIApB Reagent offers a vibrational fingerprint that supports the functional group designations. The stretching vibrations of the O-H and N-H groups overlap, resulting in a wide absorption band at 3236-3412 cm^{-1}. Aromatic C-H stretching shows at 3174 cm^{-1}. The azo linkage (-N=N-) is confirmed by a distinctive band at 1454 cm^{-1}. The peak at 1670 cm^{-1} indicates the C-O stretching of the phenol, whereas the band at 752 cm^{-1} identifies the ortho-disubstituted benzimidazole ring [14, 15].

The functional groups of BATA were identified by FTIR spectrum. The stretching vibrations of the O-H group overlap, creating a broad absorption band at 3444 cm^{-1}. The C=N group appears at 1620 cm^{-1}. Also, aromatic CH_3-C-H stretching is observed at 2961 cm^{-1}. A prominent band at 1463 cm^{-1} confirms the azo linkage (-N=N-). The peak at 1589 cm^{-1} represents the C=C stretching, while the band at 752 cm^{-1} defines the C-S group [27-30].

The BIApB and BTAT UV-Vis absorption spectra show significant and distinct peaks. The BIApB spectrum appears as one strong band at 440 nm. It is associated with the (π - π *) transition in the heterocyclic part and also with the (n- π *) electron transfer, including the (-C=N-) component [25]. Furthermore, BTAT occurs as a single broad band at 430 nm. This peak belongs to the (π - π *) transformation in the heterocyclic section, in addition to the (n- π *) electron transfer containing the (-C=N- and -C=S-) groups [26]. During the analysis of the gold coordination spectra, the shape and density of the absorption ranges were changed. The absorption spectra of the two complexes were identified as charge-transfer spectra. In aqueous solution, gold

complexes with BIApB and BTAT showed absorption maxima at 490 nm and 470 nm, respectively. While in CPL, gold complexes with novel reagents BIApB or BTAT show an absorption maximum at λ_{max} of 584 nm and 526 nm for both reagents, respectively. The red shift was made by coordinate with gold in the presence of micelles mediate [25].

The resultant molecule is promising for the possible creation of a CPE method. When complexes are produced without a surfactant, they are difficult to remove because of the presence of electronic pair azo, imidazole, and thiazole groups in the ligand. Because the development of the complex necessitates the addition of a surfactant, the CPE strategy looks to be the most promising. To achieve maximal sensitivity and accuracy of extraction, numerous basic factors were studied, such as pH, surfactant amounts, temperature for CPL creation, and other significant variables [26].

Figure 2 depicts the UV-Vis and FTIR spectra for the novel ligands and gold complexes.

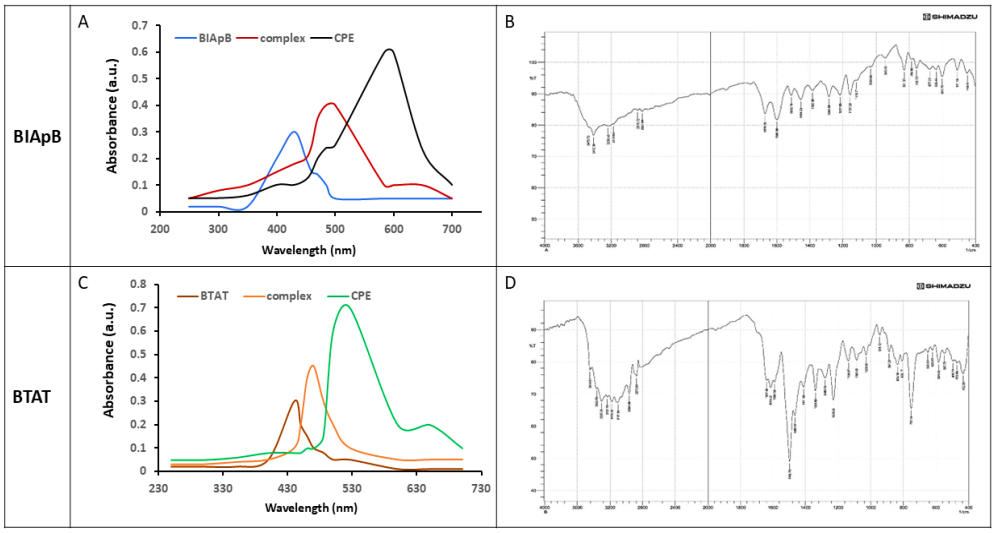

Figure 2. Spectral analysis of the synthesized BIApB and BTAT ligands and their gold complexes. (A) UV-Vis absorption spectra for the BIApB ligand, its Au (III) complex, and the resulting phase after CPE procedure. (B) FTIR spectrum of the purified BIApB reagent. (C) UV-Vis absorption spectra for the BTAT ligand, its Au (III) complex, and the CPE phase. (D) FTIR spectrum of the purified BTAT reagent.

3.2. Stoichiometry studies of gold complexes

Figure 3 shows the stoichiometry of gold complexes containing two distinct ligands, BIApB and BTAT. This study employed two analytical methods: the slope-ratio method and the molar-ratio method. Figures 3A and 3C use the slope-ratio approach, which involves graphing the logarithm of the distribution coefficient (log D) vs. the logarithm of the ligand concentration. In these figures, the slope of the resulting straight line corresponds to the ligand's stoichiometric coefficient. The slope for the BIApB ligand in Figure 3A is around 1.01, while for the BTAT ligand in Figure 3C it is roughly 1.06. The two values suggest that the gold complexes have a metal-to-ligand ratio of 1:1.

Additionally, **Figures 3B and 3D** present the results of the molar-ratio method, where the absorbance of the complex is measured while varying the molar ratio of the ligand to the metal (CL/CM). In this method, the stoichiometry is determined by the intersection point of two tangent lines drawn from the initial rising portion and the final plateau of the curve. For both BIApB (**Figure 3B**) and BTAT (**Figure 3D**), the intersection occurs at a CL/CM value of 1. This confirms that the complex reaches its maximum formation when the ligand and gold are present in an equal molar ratio. Collectively, both methods provide consistent evidence that gold forms a stable 1:1 complex with these specific ligands.

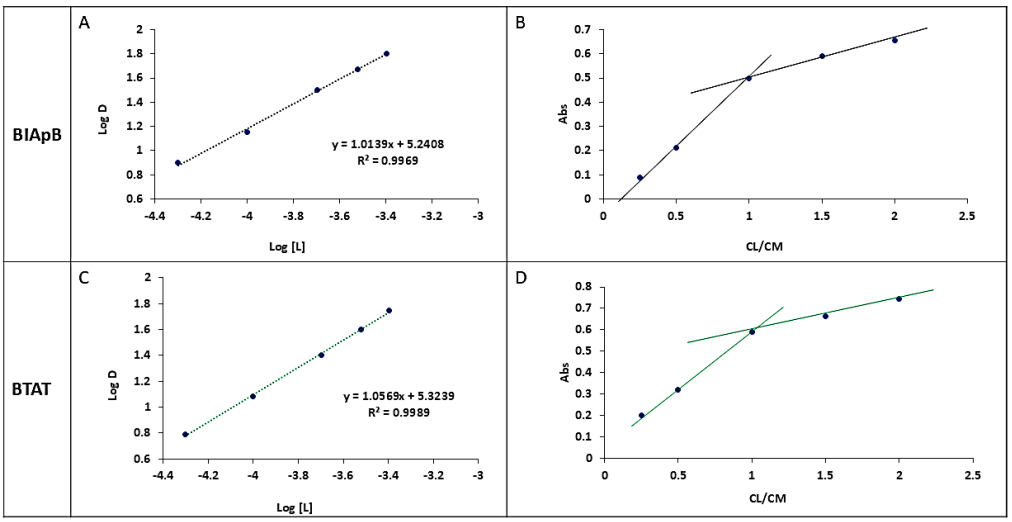

Figure 3. Stoichiometric determination of gold complexes with BIApB and BTAT ligands: (A) the slope-ratio method for the Au-BIApB complex, (B) the molar-ratio method for the Au-BIApB complex, (C) the slope-ratio method for the Au-BIApB complex, and (D) the molar-ratio method for the Au-BTAT complex.

3.3. Optimization of CPE procedure

The highest absorption of gold complexes occurs at pH 8 and 10, as shown in **Figure 3A**. The drop in effectiveness of absorption in a severely acidic solution is most likely due to ligand protonation. Whereas the decrease at higher pH levels is ascribed to the gold ion's shift into fewer reactive compounds. To effectively link Au (III) to colored complexes with the two chelators, about 1×10^{-4} mol L^{-1} of ligands are required. To separate Au (III) more efficiently, add 1×10^{-4} mol L^{-1} of the two ligands (BIApB and BTAT) to generate combinations and CPL.

Using 0.5 or 0.8 mL of Triton X-100, a non-ionic surfactant, proved to be most successful (**Figure 4B**). At lower amounts of Triton X-100, the resulting micellar layer is insufficient for full extraction of the colored complexes, whereas at higher levels, a greater quantity of CPL appears, lowering the amount of the Au complexes in it and, as a consequence, decreasing the analytical signal. To hasten the separation of the aqueous and CPL, both complexes must be heated for 15 minutes (**Figure 4C**). Furthermore, the optimal temperatures for both complexes were determined to be 80° C (**Figure 4D**).

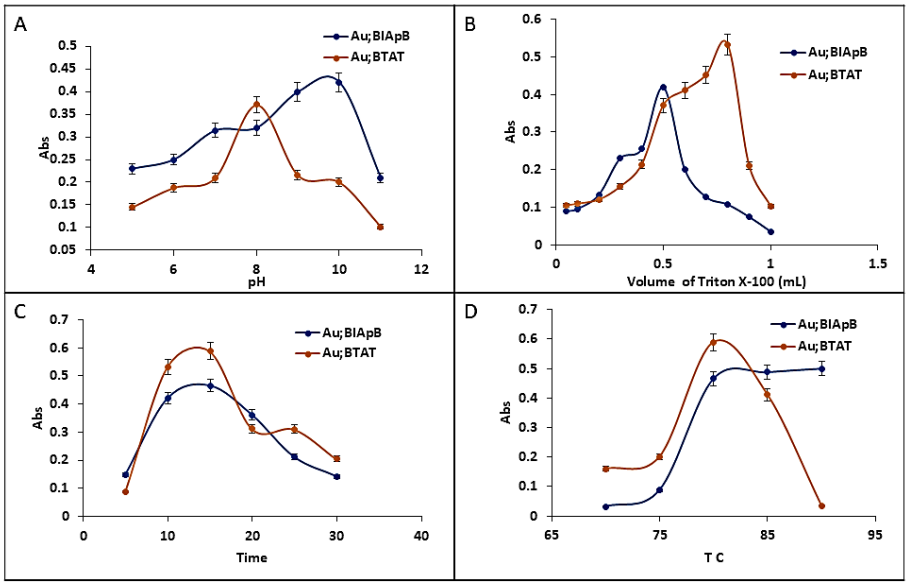

Figure 4: Optimization of experimental factors for Au-BIApB and Au-BTAT complexes: (A) pH, (B) Triton X-100 volume, (C) heating time, and (D) temperature on the absorbance of optimum complex formation for both gold-based analytes.

3.4. Thermodynamic study

The thermodynamic parameters, and equilibrium extraction constants (K_{ex}) for the extraction of the [Au-BIApB] and [Au-BTAT] ion pair complex during the CPE are established. The equation (1) is used to calculate the K_{ex}. These thermodynamic constants reflect the cumulative effect of all equilibrium processes governing the separation, including the distribution of the analyte between the aqueous and surfactant (micelle) phases, the association constant driving complex formation, the micelle aggregation constant as a function of temperature, and the transfer of the ion-pair complex from the aqueous phase to the surfactant phase [29,30].

The thermodynamic parameters, the enthalpy change (ΔHex), the Gibbs free energy values (ΔGex), and the entropy values (ΔSex) were calculated. These parameters were summarized in **Table 1** and derived from the slope and intercept of the linear relationship between log K_{ex} and 1/T (Van't Hoff plot) [30].

$$K_{ex} = \frac{D}{[M^{n+}]\,[L]} \quad \ldots \qquad (2)$$

Table 1. Thermodynamic data for extraction Au (III) in different temperatures.

TC°	TK°	BIApB			BTAT		
		ΔH_{ex} KJ mol^{-1}	ΔG_{ex} KJ mol^{-1}	ΔS_{ex} J	ΔH_{ex} KJ mol^{-1}	ΔG_{ex} KJ mol^{-1}	ΔS_{ex} J
70	343		-51.04985	148.8338		-54.4968	158.8833
75	348		-53.94973	155.0284		-56.5228	162.4224
80	353	15.70	-59.87067	169.6057	15.91	-60.7352	172.0549
85	358		-61.12679	170.7456		-59.1195	165.1388
90	363		-62.55996	172.3419		-57.9634	159.6794

3.5. Interferences effect

Table 2 evaluates the selectivity of the extraction process by measuring the impact of various foreign ions on the E% and distribution ratio (D) of Au (III) complexes using BTAT and BIApB. For both complexes, the E% remains remarkably high across all tested interferences, with values generally exceeding 93%. Specifically, Cr^{3+}, Hg^{2+}, and Ni^{2+} show the highest extraction efficiencies, often surpassing 98%, which indicates that these ions do not significantly hinder the formation or recovery of the gold complexes.

In contrast, Cd^{2+} and Co^{2+} result in slightly lower E% values and higher absorbance readings compared to the other ions, suggesting a minor competitive effect, though the efficiency still remains robust. Overall, the high D values and consistent E% show that the proposed extraction procedures for BTAT and BIApB are very selective and effective for Au (III) recovery, even in the presence of a variety of metallic interferences.

Table 2. The Impact of Interference on extraction efficiency of Au(III) complexes

Interferences	BIApB			BTAT		
	Abs	D	E%	Abs	D	E %
Cd^{2+}	0.59	23.47	95.91	0.089	14.20	93.42
Cr^{3+}	0.29	61.70	98.40	0.02	117.03	99.15
Hg^{2+}	0.28	65.15	98.48	0.027	69.0	98.57
Ni^{2+}	0.30	58.63	98.32	0.026	73.32	98.65
Co^{2+}	0.66	20.42	95.33	0.077	16.91	94.41

3.6. Analytical figures of CPE procedure

Also, **Table 2** summarizes the analytical figures of merit for the designed CPE process under perfect circumstances. The precision and accuracy of the proposed CPE method were tested using 6 tests at two

amounts of Au (III) (8.0 and 15.0 μg L^{-1}) during two consecutive days. The relative standard deviations (RSD%) ranged 8.7% and 1.1%. Precision was evaluated in terms of repeatability and expressed as the RSD%. It is calculated using the standard deviation (S) of replicate measurements and the mean value ($\bar{x}$), in the equation 3:

$$\text{RSD } \% = \frac{s}{\bar{x}} \times 100 \quad (3)$$

The efficacy of this method was evaluated employing linearity, limit of detection (LOD), limit of quantification (LOQ), pre-concentration factor (PF), and enrichment factor (EF). The results were obtained using equations (4-7). The calibration curve was created by graphing the absorbance vs. the quantity of gold ions. Linearity was achieved over 1.0-7.0 μg L^{-1} using a 10 mL sample volume for both complexes. The International Union of Pure and Applied Chemistry (IUPAC) defined LOD and LOQ as the standard deviation of the blank (σ sigma) and the slope of the calibration curve (S), respectively.

$$\text{LOD} = \frac{3\,\sigma}{S} \quad (4)$$

$$LOQ = \frac{10\,\sigma}{S} \quad (5)$$

The LOD and LOQ were 0.30 and 0.35 μg L^{-1}, respectively, the Au-BIApB and Au-BTAT complexes indicating high sensitivity for trace analysis. The efficiency of the extraction is characterized by the pre-concentration factor (PF) and the enrichment factor (EF). The PF is defined as the ratio of the initial sample volume (V_{sample}) to the volume of the CPL (V_{CPL}). The Enrichment Factor (EF), which quantifies the increase in sensitivity, is calculated as the ratio of the slope of the calibration curve obtained with CPE ($S_{with\ CPE}$) to the slope obtained without pre-concentration ($S_{without\ CPE}$). The highest PF achieved was 200 and 125 for the Au-BIApB and Au-BTAT complexes, confirming significant concentration of the analyte. **Table 3** summarizes the analytical parameters for the proposed CPE procedure.

$$\text{PF} = \frac{V_{sample}}{V_{CPL}} \quad (6)$$

$$\text{EF} = \frac{S_{with\ CPE}}{S_{without\ CPE}} \quad (7)$$

Table 3. Figures of merit for the determination of Au (III) with BIApB and BTAT by the suggested techniques

Parameter	BIApB	BTAT
λ_{max} (nm)	584	526
Regression equation with CPE procedure	y=0.2942x+0.0362	y=0.3243x+0.0522
Correlation coefficient (R)	0.997	0.996
Concentration range (μg L^{-1})	1-7	1-7
LOD (μg L^{-1})	0.30	0.35
LOQ (μg L^{-1})	1.0	1.16
Sandell's sensitivity (μg cm^{-2})	9.397×10^{-5}	1.005×10^{-4}
Molar absorptivity ($L.mol^{-1}.cm^{-1}$)	2833	3086
Composition of complex (M: L)	2:1	2:1
RSD% (n=6)	8.7	1.1
Preconcentration factor	200	125
Enrichment factor	7.86	14.40

4. Comparison with other studies

The proposed procedure (CPE/UV-Vis) provides a highly precise and cost-effective alternative to conventional gold detection methods. UV-Vis spectrophotometry, rather than expensive atomic spectroscopy (such as ICP or EAAS), lowers operational expenses while maintaining good performance. Its key strength is enhancement factors (125 and 200), which efficiently concentrates trace gold to levels comparable to far more expensive procedures. The detection limit (0.3 μg L^{-1}) is not as low as the specialized EAAS approach, but it surpasses numerous common FAAS methods, making it extremely useful for environmental monitoring.

Additionally, it operates under alkaline conditions (pH 8 or 10), providing a unique chemical alternative to the highly acidic environments required by most previous studies. The compassion analysis was given in **Table 4**.

Table 4. Comparison of the suggested approach to previous pre-concentration procedures for gold determination.

Method	Sample	Extractant	pH	LOD (µg L^{-1})	EF, PF	Linearity (µg L^{-1})	RSD%	Ref.
SS-IP-DLLME/FAAS	Water, cosmetic	213 µL 1-octanol, 1550 µg Aliquat336	2.5	0.10	280	0.2–300	1.89	[5]
SE/ ICP-AES	Water	500 g L^{-1} DES (Lidocaine + decanoic acid)	1.0	-	-	-	-	[6]
SPE/FAAS	Water	THIOPAM-SG /3.0% thiourea	1.55	0.38	50	0.1-52.1	2.8	[7]
DLLME/ FAAS, and ICP-OES	Water, sediment	1.2 mL acetonitrile	4	1.0	47, 44	2-12	0.417–3.56	[12]
IL-DLLME/FAAS	Water	1.2 mL [C_nMIM]Br	1.8	0.13	23.7	0.9–400		[29]
CPE/EAAS	Water	PONPE 7.5	2	0.002	200	0.01–0.2	3.6	[30]
CPE/FAAS	Geological	(0.5%) Triton X-114	1	1.5	31	5-1000	4.36	[32]
CPE/FAAS	mine samples	0.4 (w/v%) PONPE 7.5	2	3.8	16	-	1.4	[34]
CPE/ UV-Vis	-	Triton X-100, Au-BIApB and Au-BTAT	8 10	0.3, 0.35	200, 125	1.0-7.0	8.7, 1.1	This study

Electrothermal atomic absorption spectroscopy (EAAS)
Ionic liquid dispersive liquid-liquid microextraction (IL-DLLME)
N-((6-(2-thienyl)pyridin-2-yl) methyl)propan-1-amine to the surface of silica (THIOPAM-SG).
polyethyleneglycolmono-*p*-nonylphenylether (PONPE 7.5)
Solid phase extraction (SPE)
Syringe–Syringe Ion Pair-Dispersive Liquid-Liquid Microextraction (SS-IP-DLLME)

5. Biological Activity

This study investigated the biological activity of two new organic reagents (BIApB and BTAT) and their complexes prepared with Au (III). The results are shown in the **Table 5** for two types of pathogenic bacteria. The bacteria were cultured in Mueller-Hinton agar at 37° C. These bacteria are Escherichia coli and Staphylococcus aureus. The results attached in the tables below show that the tested compounds have a high inhibitory capacity for Gram-positive and Gram-negative bacteria were used, and it was observed that the Diameter of inhibition increases with increasing concentration of the substance [27-30].

Table 5. Measurement of the inhibition diameter of the two organic reagents, BIApB and BTAT, with the gold-complex with the bacteria under study

BIApB					
Bacteria	Aurate compound				t –test
concentration	100	200	300	Control	Sd=6.22 N=4, df=3
E- coli G(-Ve) mm	8	0	0	0	tcal= 2.25
StapH G(+Ve) mm	12	10	14	0	tcrit at 95%=3.182 p-value =0.05
BTAT					
Bacteria	Aurate compound				t –test
Concentration	100	200	300	Control	Sd=2.22 N=4, df=3
E- coli G(-Ve) mm	19	21	23	0	tcal= 2.48
StapH G(+Ve) mm	21	25	28	0	tcrit at 95%=3.182 p-value =0.05

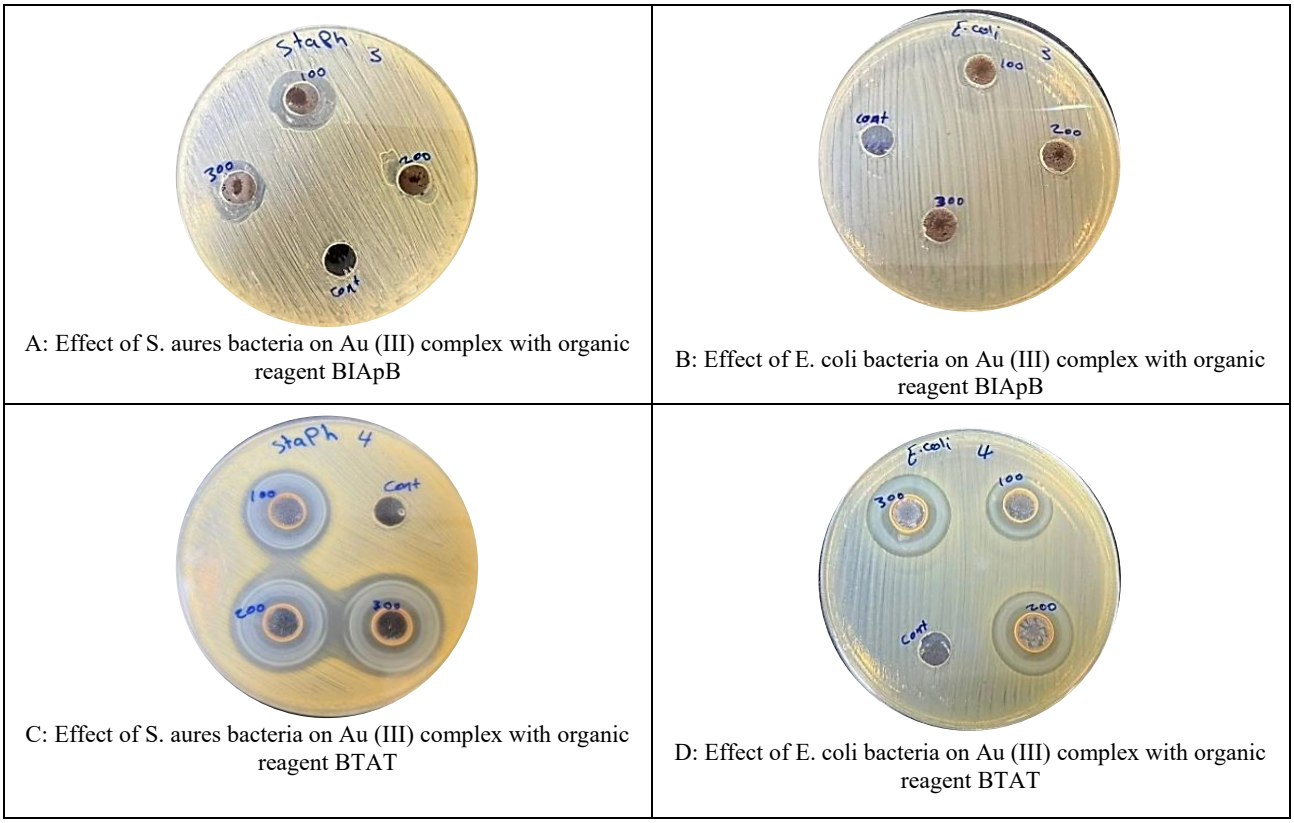

A: Effect of S. aures bacteria on Au (III) complex with organic reagent BIApB

B: Effect of E. coli bacteria on Au (III) complex with organic reagent BIApB

C: Effect of S. aures bacteria on Au (III) complex with organic reagent BTAT

D: Effect of E. coli bacteria on Au (III) complex with organic reagent BTAT

Figure 5. The biological activity of the Au (III) complexes was assessed against *S. aureus* and *E. coli*.

6. Conclusion

This study shows the comparative efficiency of two novel azo-ligands, BIApB and BTAT, as chelating agents for the CPE of Au (III). This technique was effectively used to determine gold as an ion-pair-associated complex, with novel chelators ensuring efficient metal transfer to the organic layer. This study shows that BIApB and BTAT are capable of extracting Au (III) in conjunction with well-known ligands, providing a straightforward, effective, and green technique for their preconcentration and characterization. This enhanced potency is attributed to the presence of the sulphur atom in the benzothiazole ring, which increases the lipophilic character and membrane permeability of the complex. Statistical validation using a t-test confirmed a dose-dependent biological response for both complexes. Ultimately, the findings highlight BTAT as a multifunctional reagent, offering high sensitivity for gold determination alongside significant antimicrobial potential. The antibacterial screening revealed that the BTAT-Au(III) complex is a superior antibacterial agent compared to the BIApB-Au(III) complex. The enhanced activity of BTAT, particularly its ability to inhibit *E. coli* where BIApB failed, can be attributed to the presence of the benzothiazole moiety. The sulphur atom in the BTAT scaffold likely increases the lipophilicity of the complex, facilitating better penetration through the bacterial peptidoglycan layers and subsequent interaction with intracellular proteins. In the future, these reagents may be used in real sample analysis, mechanism of bioactivity, and others.

Conflict of interest

The authors declare no conflict of interest.

References

1. P. Poormoghadam, S. Bahar, and Y. Naghdi, “Recovery of Au (III) from electronic waste using solid phase extraction based on a magnetic nanobiocomposite, OCBs@ Fe3O4@ UiO-66-SH,” Microchim. Acta, vol. 192, no. 6, p. 382, 2025.

2. H. Serbest, S. Bakırdere, and S. Keyf, “Determination of gold at trace levels in gold plating wastewater samples by vortex-assisted amidosulfonic acid-coated magnetic nanoparticle-based solid-phase microextraction method prior to slotted quartz tube flame atomic absorption spectrometric measurements,” Chem. Pap., vol. 76, no. 6, pp. 3437 – 3445, 2022.
3. V. Maksimova, V. Lapina, L. Martynov, A. Shishov, and O. Mokhodoeva, “Gold determination by electrothermal atomic absorption spectrometry after preconcentration using natural deep eutectic solvent based on menthol and camphor,” J. Anal. Test., vol. 7, no. 4, pp. 435 – 443, 2023.
4. B. Zawisza, R. Sitko, and A. Gagor, “Determination of ultra-trace gold in cosmetics using aluminum-magnesium layered double hydroxide/graphene oxide nanocomposite,” Talanta, vol. 245, p. 123460, 2022.
5. R. O. Omondi, S. O. Ojwach, and D. Jaganyi, “Review of comparative studies of cytotoxic activities of Pt (II), Pd (II), Ru (II)/(III) and Au (III) complexes, their kinetics of ligand substitution reactions and DNA/BSA interactions,” Inorganica Chim. Acta, vol. 512, p. 119883, 2020.
6. W. A. Soomro et al., “Development of a dispersive liquid – liquid microextraction technique for ultra-sensitive detection of gold in environmental samples using atomic absorption spectrometry,” Environ. Monit. Assess., vol. 197, no. 3, p. 235, 2025.
7. R. Juvonen, T. Lakomaa, and L. Soikkeli, “Determination of gold and the platinum group elements in geological samples by ICP-MS after nickel sulphide fire assay: difficulties encountered with different types of geological samples,” Talanta, vol. 58, no. 3, pp. 595 – 603, 2002.
8. X. Tang, B. Li, J. Lu, H. Liu, and Y. Zhao, “Gold determination in soil by ICP-MS: comparison of sample pretreatment methods,” J. Anal. Sci. Technol., vol. 11, no. 1, p. 45, 2020.
9. L. Tavakoli, Y. Yamini, H. Ebrahimzadeh, A. Nezhadali, S. Shariati, and F. Nourmohammadian, “Development of cloud point extraction for simultaneous extraction and determination of gold and palladium using ICP-OES,” J. Hazard. Mater., vol. 152, no. 2, pp. 737 – 743, 2008.
10. A. S. Amin, “Utility of solid phase extraction for spectrophotometric determination of gold in water, jewel and ore samples,” Spectrochim. Acta Part A Mol. Biomol. Spectrosc., vol. 77, no. 5, pp. 1054 – 1058, 2010.
11. R. Lupu, A. Nat, and A. Ene, “Determination of gold in Romanian auriferous alluvial sands and rocks by 14 MeV neutron activation analysis,” Nucl. Instruments Methods Phys. Res. Sect. B Beam Interact. with Mater. Atoms, vol. 217, no. 1, pp. 123 – 135, 2004.
12. J. L. Manzoori, H. Abdolmohammad-Zadeh, and M. Amjadi, “Simplified cloud point extraction for the preconcentration of ultra-trace amounts of gold prior to determination by electrothermal atomic absorption spectrometry,” Microchim. Acta, vol. 159, no. 1, pp. 71 – 78, 2007.
13. W. S. El-Naggar, T. A. Lasheen, E.-S. A. Nouh, and A. K. Ghonaim, “Cloud point extraction and preconcentration of gold in geological matrices prior to flame atomic absorption determination,” Cent. Eur. J. Chem., vol. 8, no. 1, pp. 34 – 40, 2010.
14. R. A. B. Aldujaili, R. A. Ghafil, H. F. Mohsein, F. A. Wannas, E. A. Azooz, effective design, spectroscopic characterization, antifungal activity, and computational analysis of new pyrazole and tetrazole derivative compounds, Bulletin of the Chemical Society of Ethiopia, 2026, 40,2, 271 – 281. https://www.ajol.info/index.php/bcse/article/view/314761.
15. E. A. Azooz, A. Y. M. Al-Murshedi, A. A. M. Abodiame, G. J. Shabaa, N. K. El Abbadi, and D. Snigur, “A novel green cloud point extraction-based switchable hydrophilicity solvent method for antimony separation and quantification from various bottled beverages by HGAAS,” Microchem. J., vol. 207, p. 111824, 2024.
16. Z. Bahadir, “A surfactant-based emulsification microextraction (SBEME) method for the atomic absorption determination of gold,” Desalin. Water Treat., vol. 169, pp. 305 – 311, 2019.
17. F. Abd Wannas, E. A. Azooz, R. K. Ridha, and S. K. Jawad, “Separation and micro determination of zinc (II) and cadmium (II) in food samples using cloud point extraction method,” Iraqi J. Sci., pp. 1049 – 1061, 2023.
18. R. K. Ridha, E. A. Azooz, and S. S. Taresh, “Rapid palladium preconcentration and spectrophotometric determination in water and soil samples,” 2022.
19. S. Bharti, “Recent advances in heavy metal removal from wastewater using nanomaterials and cloud point extraction: A comprehensive review,” Int. J. Environ. Sci. Technol., vol. 22, no. 6, pp. 5057 – 5084, 2025.
20. E. A. Azooz, F. A. Wannas, and S. K. Jawad, “Developed cloud point extraction coupled with onium system for separation and determination cobalt in biological samples,” Res. J. Pharm. Technol., vol. 14, no. 2, pp. 594 – 598, 2021.

21. E. A. Azooz, J. R. Moslim, and S. K. Jawad, “cloud point extraction methodology for separation, extraction and preconcentration of Mn (VII) coupled with spectroscopy for determination in different samples.,” Biochem. Cell. Arch., vol. 20, no. 1, 2020.
22. K. J. Shawket, M. O. Kadhim, and E. A. Azooz, “Incorporation onium system with cloud point extraction method for extraction and determination Iron (III) and Mercury (II) in different samples,” Orient. J. Chem., vol. 33, no. 4, p. 1879, 2017.
23. S. K. Jawad, M. U. Kadhium, and E. A. Azooz, “Separation and spectrophotometric determination of iron (III) and mercury (II) via cloud point extraction with new azo-derivative,” Eurasian J. Anal. Chem., vol. 13, no. 5, pp. 1 – 11, 2018.
24. S. K. Jawad, M. U. Kadhium, and E. A. Azooz, “Application cloud point extraction method joined with liquid ion exchange for selective determination of Fe3+ and Hg2+ in real samples,” J Eng Appl Sci, vol. 14, no. 11, pp. 3514 – 3521, 2019.
25. K. J. AL-Adilee, A. K. Abass, and A. M. Taher, “Synthesis of some transition metal complexes with new heterocyclic thiazolyl azo dye and their uses as sensitizers in photo reactions,” J. Mol. Struct., vol. 1108, pp. 378 – 397, 2016.
26. D. A. Al-Yousefi and I. R. Ali, “Spectrophotometric determination of transition elements by cloud point extraction with use laboratory by thiazol azo reagent and applied in environmental samples,” in AIP Conference Proceedings, AIP Publishing LLC, 2022, p. 30007.
27. L. A. Ibrahim and R. A. B. Aldujaili, “Novel Thiadiazole Derivatives: Preparation, Identification, and Analysis of Their Antioxidant Activity,” Rev. Adv. Chem., vol. 15, no. 3, pp. 128 – 138, 2025.
28. R. B. Shakuntala, J. Keshavayya, H. Nagarajappa, Y. S. Naik, and I. Pushpavathi, “Synthesis, characterization and geometrical optimization of azo dyes derived from the substituted pyrazole and benzothiazole amines coupled with 3-N, N-diethyl amino phenol,” J. Mol. Struct., vol. 1343, p. 142802, 2025.
29. V. Travica, O. Šovljanski, T. Erceg, and M. Perovi, “Updating the Status quo on the Eco-Friendly Approach for Antioxidants Recovered from Plant Matrices Using Cloud Point Extraction,” 2024.
30. S. Ali and I. R. Ali, “Cloud point extraction and determination of Nickel (II) ions complex in real samples using New azo reagent,” Adv. Sci, vol. 1, no. 2, pp. 7 – 18, 2020.